

University of Nebraska - Lincoln

DigitalCommons@University of Nebraska - Lincoln

---

Faculty Publications from the Department of  
Electrical and Computer Engineering

Electrical & Computer Engineering, Department of

---

8-20-2007

# Spatial confinement effects in laser-induced breakdown spectroscopy

X. K. Shen

*University of Nebraska - Lincoln*

Jian Sun

*University of Nebraska - Lincoln, jsun3@unl.edu*

Hao Ling

*University of Nebraska - Lincoln, hling4@unl.edu*

Yongfeng Lu

*University of Nebraska - Lincoln, ylu2@unl.edu*

Follow this and additional works at: <http://digitalcommons.unl.edu/electricalengineeringfacpub>



Part of the [Electrical and Computer Engineering Commons](#)

---

Shen, X. K.; Sun, Jian; Ling, Hao; and Lu, Yongfeng, "Spatial confinement effects in laser-induced breakdown spectroscopy" (2007).  
*Faculty Publications from the Department of Electrical and Computer Engineering*. 96.  
<http://digitalcommons.unl.edu/electricalengineeringfacpub/96>

This Article is brought to you for free and open access by the Electrical & Computer Engineering, Department of at DigitalCommons@University of Nebraska - Lincoln. It has been accepted for inclusion in Faculty Publications from the Department of Electrical and Computer Engineering by an authorized administrator of DigitalCommons@University of Nebraska - Lincoln.

## Spatial confinement effects in laser-induced breakdown spectroscopy

X. K. Shen, J. Sun, H. Ling, and Y. F. Lu<sup>a)</sup>

Department of Electrical Engineering, University of Nebraska-Lincoln, Lincoln, Nebraska 68588-0511

(Received 4 March 2007; accepted 20 July 2007; published online 20 August 2007)

The spatial confinement effects in laser-induced breakdown of aluminum (Al) targets in air have been investigated both by optical emission spectroscopy and fast photography. A KrF excimer laser was used to produce plasmas from Al targets in air. Al atomic emission lines show an obvious enhancement in the emission intensity when a pair of Al-plate walls were placed to spatially confine the plasma plumes. Images of the Al plasma plumes showed that the plasma plumes evolved into a torus shape and were compressed in the Al walls. The mechanism for the confinement effects was discussed using shock wave theory. © 2007 American Institute of Physics.

[DOI: 10.1063/1.2770772]

Laser-induced breakdown spectroscopy (LIBS) has been developed as a very popular and useful elemental analysis technique in recent years. When a powerful laser beam is focused on solid, liquid, or gas targets, a luminous hot spark is generated, which is called laser-induced plasma. By spectrally analyzing the line emissions from the luminous plasma, the elemental compositions can be deduced. LIBS has such advantages as simplicity of method, little sample preparation, nearly nondestructive, real-time analysis, and simultaneous multielemental analysis. LIBS has been applied in a wide range of applications such as aerosol detections,<sup>1</sup> diagnostics of artworks,<sup>2</sup> and remote elemental analysis.<sup>3</sup> LIBS is also a potential tool for real-time radioactive material monitoring.<sup>4</sup> However, LIBS has low detection sensitivity as compared with some mass spectroscopy techniques. In order to improve the sensitivity of LIBS, some techniques, such as dual-pulse excitation<sup>5</sup> and introduction of purge gas,<sup>6</sup> have been used.

The spatial confinement of plasmas is a potential method for improving the detection sensitivity of LIBS. LIBS is usually influenced by many factors, such as the optical properties of the targets and the operating laser parameters. The generation and expansion of laser-induced plasmas are also very complex processes. Together with the plasma generation, shock waves will be produced. The expansion of laser-induced plasmas and the shock wave phenomenon have been studied by many groups. The shock wave can be observed and studied using interferometry and shadowgraphy.<sup>7</sup> The temperature and pressure can be calculated in the shock front region.<sup>8</sup> If the shock wave encounters walls during its expansion, the shock wave will be reflected and spatial confinement effects will occur. Some researchers have studied the spatial confinement effects in LIBS caused by craters. Corsi *et al.* reported that the plasmas created within the craters were confined by the crater walls.<sup>9</sup> In this work, the spatial confinement effects in LIBS were studied using a pair of plate walls. Plasma plumes were produced in between two parallel walls, which have similar functionalities as the crater walls. The distance between the two walls was 10 mm or more, which is large compared to the plume size. Nevertheless, the spatial confinement effects were still obvious.

The schematic diagram of the experimental setup used for optical emission spectroscopy is shown in Fig. 1. The laser used for plasma generation is a KrF excimer laser (Lambda Physik, Compex 205) with a wavelength of 248 nm and a pulse width of 23 ns. The laser beam was focused to a cylindrical target of Al at an incidence angle of 45° by a UV-grade quartz lens (L1) of a 15 cm focal length. The Al cylindrical target was mounted on a rotating motor in order to avoid over ablation. A pair of parallel Al-plate walls were placed to sandwich the Al target. Plasma plumes were produced at the center between the two walls. The light emissions from the luminous plasma plumes were collected using an optical fiber by a pair of UV-grade quartz lens (L2 with  $f/17$  cm and L3 with  $f/5$  cm). The plume size is around several millimeters. We only studied the optical emissions at the center of the plasmas where the continuum background emission is the strongest. The optical fiber was coupled to an echelle spectrometer (Andor Tech., Mechelle 5000). The spectrally resolved lines were detected by an intensified charge coupled device (ICCD) (Andor Tech., iStar, DH734). The ICCD camera was operated in the gated mode. The gate delay and gate width can be adjusted so that the spectra at

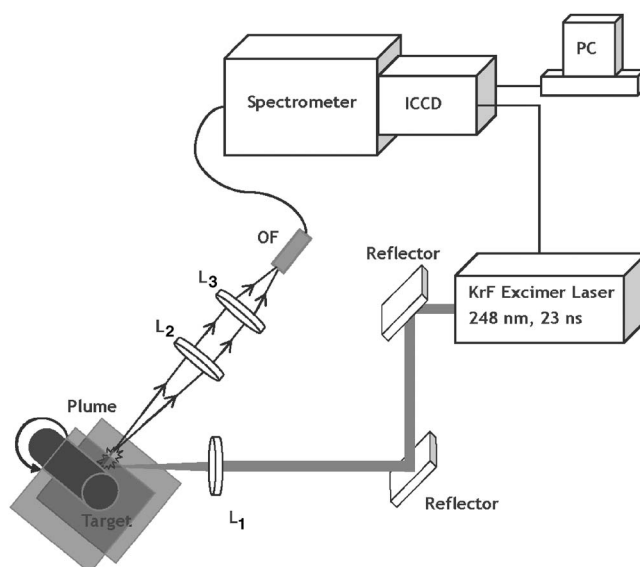


FIG. 1. Schematic diagram of the experimental setup for optical emission spectroscopy.

<sup>a)</sup> Author to whom correspondence should be addressed; electronic mail: ylu2@unl.edu

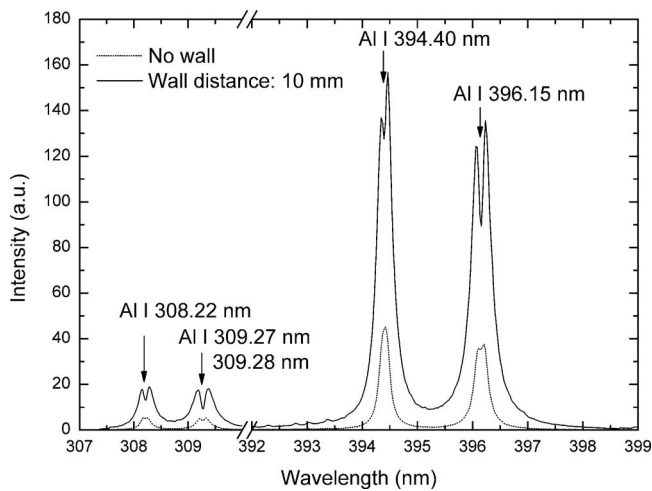


FIG. 2. Time-integrated LIBS spectra of Al target with (solid curve) and without (short dotted curve) the presence of walls.

different time delays after the laser pulse can be obtained. In fast photography experiments, a Nikon microlens (105 mm,  $f/2.8$  D) was attached to the Andor ICCD camera. The images were taken from the top of the plasma plumes with a magnification of approximately 1:1.

The time-integrated LIBS spectra of an Al target were measured with a time delay of  $8 \mu\text{s}$  after the laser pulse and a gate width of  $12 \mu\text{s}$ , which was shown in Fig. 2. The laser fluence was  $15 \text{ J/cm}^2$ . The laser was slightly defocused with a focus spot size of about  $2.8 \times 0.6 \text{ mm}^2$ . The distance between the two flat walls was 10 mm. The spectra were averaged over 60 laser pulses in order to reduce the standard deviation. The solid curve represents the spectra with the presence of the Al-plate walls and the dotted curve represents the spectra without the walls. As can be seen from Fig. 2, the Al atomic lines were significantly enhanced when the walls were present. The enhancement factor was around 4. With the presence of the walls, the Al atomic lines show some absorption peaks, which is known as self-absorption. The self-absorption effect usually occurs when the plasmas are optically thick. The transition configurations for the Al

atomic lines are  $3s^23p-3s^24s$  (Al I with 394.40 and 396.15 nm) and  $3s^23p-3s^23d$  (Al I with 308.22, 309.27, and 309.28 nm), respectively, where  $3s^23p$  is the ground state of the Al atoms. The emission intensity is proportional to the transition probability and the concentration of the excited atoms. Since the transition probability for the emission is considered to be unchanged, the enhancement effect is attributed to the increase in the concentration of the excited atoms caused by the spatial confinement of laser-induced plasmas. As the plasma is generated, the pressure in the plasma region is increased to a very high level, and the shock wave is then produced. The shock wave usually travels at a higher speed than the ordinary sound wave. When it reached the walls, the shock wave was reflected by the parallel walls and traveled back to the plasma center. As a result, the plasma was confined to a smaller size, causing the increase in the plasma temperature and density at the center region. Due to this confinement effect, the emission intensities from the plasma were enhanced. In addition, the energy of the reflected shock wave also contributed to the enhancement effect. In the case of free expansion, the energy of the shock wave just dissipated into the background air.

Since the laser-induced plasma is a pulsed source, the temporally resolved emission spectra were investigated in order to better understand the temporal evolution of the plasmas. By adjusting the time delay and gate width of the ICCD detector, the optical emission spectra at different time delays were acquired. Figure 3(a) shows the evolution of the Al atomic line (Al I with 394.4 nm) emission intensity as a function of the time delay with (solid dots and curve) and without (hollow dots and dotted curve) the presence of the walls. The distance between the walls was 10 mm. The first data point was acquired with a time delay of  $2 \mu\text{s}$  and a gate width of  $3 \mu\text{s}$ . The following data points were acquired with increasing time delays by a step of  $3 \mu\text{s}$  and a gate width of  $3 \mu\text{s}$ . As can be seen in Fig. 3(a), the emission intensity was enhanced during the period of the time delay from 6 to  $20 \mu\text{s}$  while the emission intensity without the presence of the walls decreased monotonously. The maximum en-

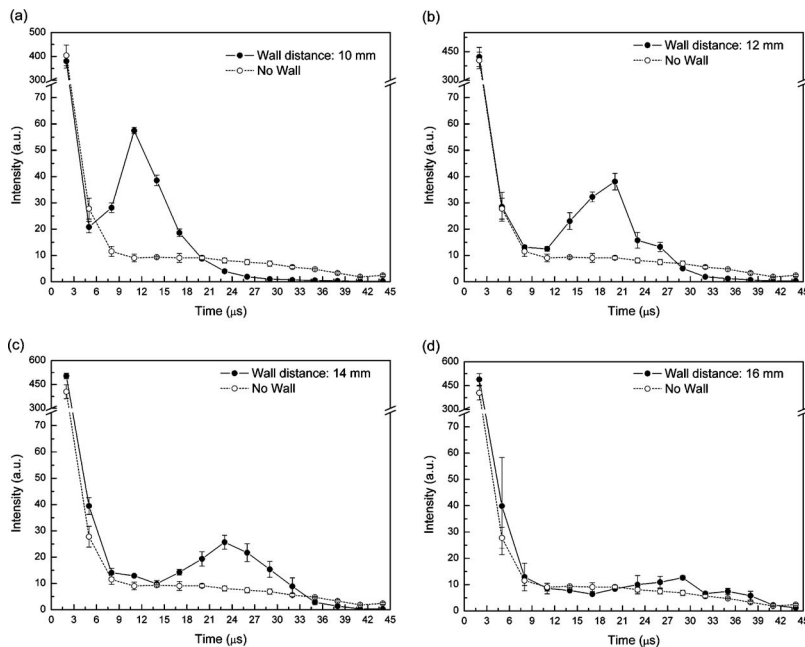


FIG. 3. Emission intensity for Al atomic lines (Al I with 394.4 nm) as a function of the time delay. The distances between the walls are (a) 10 mm, (b) 12 mm, (c) 14 mm, and (d) 16 mm, respectively.

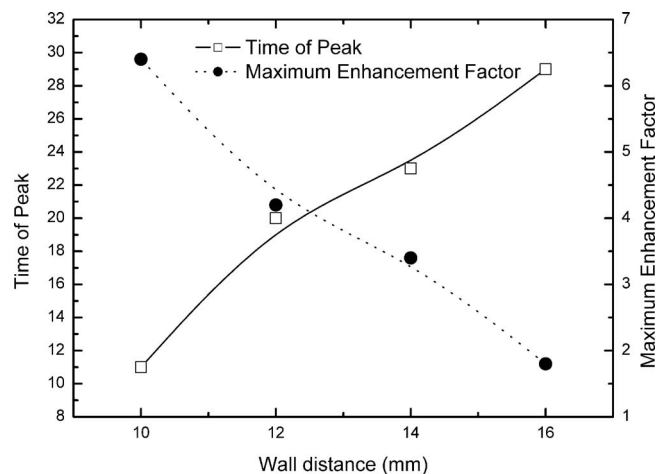


FIG. 4. Maximum enhancement factor and the time delay for the maximum enhancement as functions of the wall distance.

hancement factor was about 6 at a time delay of  $11 \mu\text{s}$  corresponding to the local peak in the figure.

As the distance between the walls increased, the temporal profile of the emission intensity changed obviously. Figures 3(b)–3(d) show the evolutions of the emission intensity as a function of the time delay with different wall distances of 12, 14, and 16 mm, respectively (solid dots and curve). They were all compared with the intensity without the walls (hollow dots and dotted curve). It is observed that the emission intensities were all enhanced although the enhancement factors depend on the wall distance. Figure 4 shows the maximum enhancement factor and the time delay for the maximum enhancement as functions of the wall distance. The maximum enhancement factor decreased and the time delay for the maximum enhancement increased as the distance increased. This is because the energy of the shock wave dissipated quickly with distance, and the traveling time increased as the wall distance increased.

Figure 5 shows the fast images on a relative intensity scale with (bottom) and without (top) the presence of the walls (10 mm in distance). The dotted ovals in the first pair of plasma images roughly indicate the focused laser spots. The first image was taken with a time delay of  $2 \mu\text{s}$  and the following images were taken with an increasing time delay by a step of  $3 \mu\text{s}$ . As can be seen from the images, the size of the luminous plasma was about 5 mm in diameter and the plasma never reached the walls. The shock waves are invisible in these pictures. As the time delay increased after  $2 \mu\text{s}$ , the plasma gradually evolved into a toroidal shape, which is possibly due to the convection effect. Sobral *et al.* have observed a similar phenomenon in laser-induced breakdown experiments in air.<sup>7</sup>

As can be seen in Fig. 5, the spatial confinement effects obviously occurred after the time delay increased to more than  $8 \mu\text{s}$ . Without the presence of the walls, the shape of the plasma plume remained nearly unchanged after the time delay of  $8 \mu\text{s}$ . With the presence of the walls, however, the plasma plume was compressed in the direction which the walls were placed, and the emission intensity at the center region increased as the time delay increased. This is consistent with the results of the optical emission spectra shown

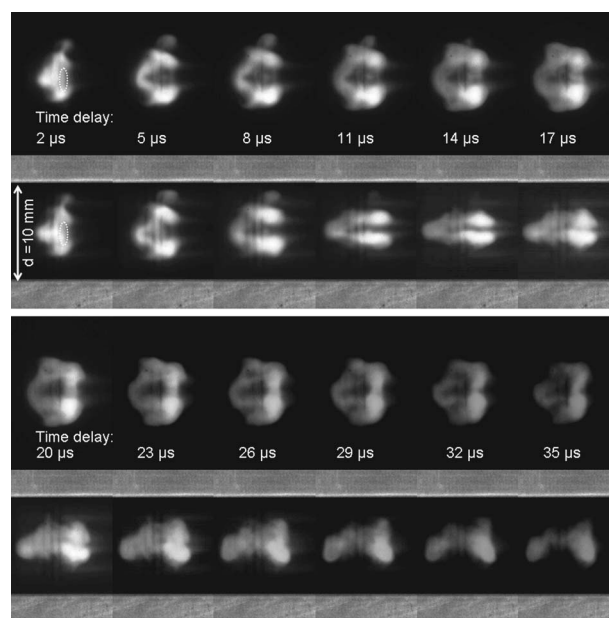


FIG. 5. Fast images of laser-induced Al plasmas with (bottom row) and without (top row) the presence of the walls.

previously. As in the previous discussion, the spatial confinement effects are attributed to the reflection and the compression of the shock wave by the parallel walls.

In summary, the spatial confinement effects in LIBS caused by a pair of Al-plate walls were investigated by optical emission spectra and fast photography. The significant enhancement in Al atomic line emissions was observed. The maximum enhancement factor for the Al atomic lines was measured to be about 6 at a time delay of  $11 \mu\text{s}$  when the distance of the walls was 10 mm. The maximum enhancement factor decreased and the time delay for the maximum enhancement increased as the wall distance increased. The spatial confinement effects are attributed to the reflection and compression of the shock wave by the walls. This simple approach of placing walls around the plasma has the potential to improve the measurement sensitivity in LIBS analyses.

This research was financially supported by U.S. Department of Energy (Nuclear and Radiological National Security Program, National Nuclear Security Administration) through cooperative agreement DE-FC52-04NA25688.

- <sup>1</sup>D. W. Hahn and M. M. Lunden, *Aerosol Sci. Technol.* **33**, 30 (2000).
- <sup>2</sup>D. Angelos, S. Couris, and C. Fotakis, *Appl. Spectrosc.* **51**, 1025 (1997).
- <sup>3</sup>D. A. Cremers, J. E. Barefield, and A. C. Koskelo, *Appl. Spectrosc.* **49**, 857 (1995).
- <sup>4</sup>J. P. Singh, F. Y. Yueh, H. Zhang, and K. P. Karney, *Rec. Res. Dev. Appl. Spectrosc.* **2**, 59 (1999).
- <sup>5</sup>J. Scaffidi, J. Pender, W. Pearman, S. R. Goode, B. W. Colston, J. C. Carter, and S. M. Angel, *Appl. Opt.* **42**, 6099 (2003).
- <sup>6</sup>S. Nakamura, Y. Ito, K. Sone, H. Hiraga, and K. I. Kaneko, *Anal. Chem.* **68**, 2981 (1996).
- <sup>7</sup>H. Sobral, M. Villagrán-Muniz, R. Navarro-González, and A. C. Raga, *Appl. Phys. Lett.* **77**, 3158 (2000).
- <sup>8</sup>L. I. Sedov, *Similarity and Dimensional Methods in Mechanics* (Cleaver Hume, London, 1959).
- <sup>9</sup>M. Corsi, G. Cristoforetti, M. Hidalgo, D. Iriarte, S. Legnaioli, V. Palleschi, A. Salvetti, and E. Tognoni, *Appl. Spectrosc.* **59**, 853 (2005).